Received: December 13, 2022. Revised: February 21, 2023.

International Journal of
Intelligent Engineering & Systems

http://www.inass.org/

Single Phase UPQC Integrated with Photovoltaic System without DC-Link Capacitor Using Fuzzy Logic Controller for Power Quality Improvement

Amirullah Amirullah[1]* **Adiananda Adiananda[1]**

[1]*Electrical Engineering Study Program, Faculty of Engineering, Universitas Bhayangkara Surabaya, Surabaya 60231, Indonesia*
* Corresponding author's Email: amirullah@ubhara.ac.id

Abstract: This paper proposed a single-phase unified power quality conditioner (UPQC) integrated by a photovoltaic (PV) array using a fuzzy logic controller (FLC) in a single-phase low-voltage 220 V-50 Hz distribution system to improve the power quality. The PV array consists of several PV panels with a maximum power of 12 kW. There are two proposed circuit configuration models, i.e. UPQC-PV connected to a linear load (LL) and UPQC-PV connected to a non-linear load (NLL). The proposed single-phase UPQC-PV is without using a DC link capacitor. The PV system is then used as a DC voltage source which functions to supply load active power when the source is interrupted and simultaneously replaces the role of the DC link capacitor to keep the PV output voltage and also the DC link connected to UPQC so that the value remains constant. FLC is used to overcome the weakness of the proportional-integral (PI) control method in determining the optimum parameters of the proportional constant and integral constant. There are six disturbances simulations i.e. Operating Mode (OPM) 1 (S-Sag-LL), OPM 2 (S-Swell-LL), OPM 3 (S-Inter-LL), OPM 4 (S-Sag-NLL), OPM 5 (S-Swell-NLL), and OPM 6 (S-Inter-NLL). In the single-phase system using UPQC-PV configuration, OPM 6 disturbance with FLC control is able to result in the lowest load voltage change. In the same configuration as the OPM 1 to OPM 6 disturbances, the FLC is able to produce a lower load voltage total harmonics distortion (THD) and source current THD than the PI control, and has complied with IEEE-519 limits. In the same configuration as PI/FLC control, OPM 4, OPM 5, and OPM 6 disturbances are able to absorb greater load active power than systems with OPM 1, OPM 2, and OPM 3 disturbances.

Keywords: Power Quality, Single-Phase UPQC-PV, FLC, PI, THD.

1. Introduction

Apart from being able to produce electric power, PV generators also produce voltage/current disturbances, harmonics or THD due to PV integration, the presence of electronic converters, and the increase in the number and capacity of NLLs, which causes a decrease in power quality. To overcome these disturbances, UPQC was used, which functions to compensate for power quality problems in terms of source voltage/load current. UPQC is a combination of series active filters (SeAF) and shunt active filter (ShAF) connected in parallel to function as a superior control over power quality problems simultaneously [1, 2]. The UPQC control method for controlling the quality of the load voltage and the quality of the source current due to simultaneous NLLs and sensitive loads has been investigated by a number of researchers. In [3], It has been examined feedback control on single-phase UPQC using the linear equivalent discrete system model (EDSM) method. The single-phase UPQC control model using a Kalman filter for regulation of the output value of source voltage and distorted load current has been simulated and tested using a prototype [4]. Single-phase UPQC with smooth switching of series active filters and shunt active filters have been proposed [5]. The main switch of the circuit operates at zero-voltage-switching (ZVS) was on and the auxiliary switch operating at zero-current-switching (ZCS) was off. In [6], it has been investigated the operation and control of the Three-Leg UPQC (TL-UPQC) using the space vector modulation (SVM) method.

The control algorithm for generating reference voltage and current using second order generalized integrator-phase locked loop (SOGI-PLL) on single-phase UPQC has been investigated [7].

Single-phase UPQC based on adaptive detection control using neuron parameters has been observed [8]. The system used phase detection voltage and reference current calculated using Instantaneous Reactive Power Theory and was able to improve the quality of the load voltage and source current even though the sine wave contains harmonics. In [9], it has been investigated and tested the one-to-three-phase UPQC circuit topology in a three-phase four-conductor (3P4W) distribution system for remote areas with economic considerations. The drawback of the variations in the single-phase UPQC model and control investigated by [1-9], is that it is only able to mitigate sag/swell source voltages, distorted source voltages, NLL currents, and low input power factor. The proposed system was still not able to maintain the load voltage if an interruption voltage happened at the source bus.

An in-depth study on size, stability analysis and power flow on a distributed generation (DG) system in the form of an integrated PV system on UPQC (3Ph UPQC-PV) has been carried out [10]. Improved UPQC performance under various load, source and channel conditions has been simulated [11]. Load voltage control using a series voltage source Inverter (VSI) and source current control using a VSI shunt are able to handle power quality problems simultaneously. A single-phase UPQC control strategy using notch filters and feedback to suppress DC-link voltage ripple due to low-frequency influences has been observed [12]. Three-phase UPQC performance supplied by PV, Wind Turbine, and Hybrid PV-Wind Turbine combined with battery energy storage (BES) using FLC in six fault scenarios has been observed [13, 14].

The implementation of the method on the UPQC-BES supplied by three combinations of renewable energy generators under fault conditions of the source voltage cutoff-capable of producing an average THD of load voltage/source current is much smaller than the PI method. In [15], it has been proposed the operation and control of a three-arm single-phase UPQC without a transformer using the space vector pulse width modulation (SVPWM) method. The proposed model and control method was able to overcome the coupling problem caused by the joint arm switch. An increase in load active power transfer using UPQC-PV-BES with PI and FLC control has been investigated [16, 17]. In case of interruption of source voltage disconnection, the combination of UPQC-PV-BES with this method is capable of producing higher load voltage, load current, and load active power than the combination of UPQC-PV and UPQC. A three-phase UPQC control strategy using dq0 and SVPWM detection methods has been developed [18]. This strategy was able to maintain load voltage stability, maintain sinusoidal source currents, and improve the power quality of the distribution network. Improving the quality of power in PV and wind energy (PV-WE) systems connected to integrated networks with energy storage systems (ESS) and electric vehicles (EV) has been studied in depth [19]. The results showed that the power output of maximum power point tracking-photovoltaic (MPPT-PV) based on FLC produces better performance than MPPT based on an artificial neural network.

Three-phase UPQC to mitigate power quality problems in the grid and harmonic systems due to NLLs supported by PV and BES systems has been observed [20]. The UPQC control synchronization operation used a self-tuning filter (STF) integrated with the unit vector generator (UVG) technique. This method was able to provide better control over the quality of the load voltage at unbalanced and distorted source voltages compared to the synchronous reference frame-PLL (SRF-PLL) method. The DG system that integrates PV with a single-phase system to a three-phase UPQC (DG-UPQC-1PH-3PH) has been observed [21]. PV generators could inject power into the grid, serving local loads connected to the three-phase four-wire (3P3W) system, and serving rural and remote area customers supplied by a single-phase network. In [22], it has been implemented a three-phase UPQC based on a quadruple-active-bridge (QAB). This topology was able to maintain load voltage stability, maintain sinusoidal source currents, and improve the power quality of the distribution network.

This paper proposed the single-phase UPQC model integrated with PV using FLC with the Mamdani fuzzy inference system (FIS) algorithm. In contrast to previous studies applied to 3P3W/3P4W systems [10-22], the combination of UPQC with PV in this study is used in a single-phase PV distribution network, hereinafter referred to as single-phase-connected UPQC-PV at LL and NLL respectively. Also different from previous UPQC configurations [1-22], the proposed single-phase UPQC design is without using a DC link capacitor circuit. The large capacity PV is then used as a DC voltage source which functions to supply load power when the source experiences an interruption voltage.

Referring to the problems above, the main contributions of this research are: (1) Designing a single phase UPQC-PV without a DC link capacitor

connected to LL and NLL in reducing source current THD, maintaining load voltage, reducing load voltage THD, and improving load active power performance due to disturbance voltages (sag/swell and interruption) on the source bus, (2) Validation of single-phase UPQC-PV connected NLL performance with single-phase UPQC-PV connected LL without DC-link capacitor for determining the best configuration in mitigation power quality problems for the proposed model, (3) Implementation of the FLC with FIS-Mamdani on the ShAF of the single-phase UPQC-PV without DC-link to overcome the weakness of PI control in determining proportional constants (K_P) and integral constant (K_I), and (4) Validation of FLC with PI control method on single phase UPQC-PV of ShAF circuit to determine the best control method in mitigation power quality problems for the proposed model.

This paper is structured as follows. Section 2 presents the proposed method i.e. a model of a single-phase UPQC-PV without a DC-link capacitor connected to LL and NLL respectively, simulation parameters, PV generation system, SeAF, and ShAF control, as well as PI control and FLC. Section 3 presents the results and discussion i.e. load voltage, series voltage, load voltage, source current, shunt compensation current, load current, source voltage THD, load voltage THD, series voltage THD, source current THD, load current THD, shunt compensation current THD, PV output power, and power active load using FLC validated by a PI method. Observation of the results is also carried out on the percentage of voltage sag/swell and interruption voltage in the proposed circuit using FLC and PI controls. In this section, two UPQC-PV configurations each connected to a LL and NLL experiencing three OPMs at the source bus are presented and the results are verified using Matlab-Simulink. Finally, the paper is concluded in section 4.

2. Research method

2.1 Proposed Method

This study aims to improve the power quality performance of a single-phase UPQC system supplied by a PV array using FLC control in a single-phase low-voltage distribution system. The PV array consists of several PV panels with a maximum PV power of 12 kW each. There are two proposed circuit configuration models, i.e. single-phase UPQC-PV connected to a LL and NLL respectively. In contrast to previous studies, the proposed UPQC circuit does not use a DC link-capacitor circuit. The PV array is proposed and used as a DC voltage source that functions to supply load power when the source is interrupted and simultaneously replaces the role of the DC link capacitor circuit to keep the PV output voltage and at the same time the DC-link voltage connected to the UPQC so that the value is constant.

The single-phase UPQC is a combination of a single-phase SeAF and a single-phase ShAF. In this study, the single-phase SeAF circuit consists of four metal oxide semiconductor field effect transistor (MOSFET) switches $(S_1,\ S_2, S_3, and\ S_4)$ which function to inject a compensating voltage to the load bus when a sag/swell occurs on the source bus. Meanwhile, the single-phase ShAF circuit consists of four insulated gate bipolar transistor (IGBT) switches $(S_1,\ S_2, S_3,\ and\ S_4)$ which function to inject harmonic compensation current to the source bus due to the presence of NLL. The single-phase UPQC-PV system is used to maintain the load voltage so that the load bus continues to get a more stable active power supply in the event of an interruption voltage on the source bus, lowers the THD of the load voltage, and simultaneously reduces the THD of the source current. The single-phase UPQC-PV circuit is located between the load buses and is connected to the source bus (PCC) via a low voltage distribution line of 220 V and a frequency of 50 Hz. The FLC method is proposed to overcome the weakness of PI control in proportional gain (K_P) and integral gain (K_I).

The disturbances in two single-phase UPQC-PV connected to LL and NLL are described in the six operating modes (OPMs) below:

a. OPM 1 (S-Sag-LL), In OPM 1, the system is connected to a LL and the sinusoidal source experiences a 50% sag voltage. The sag voltage is generated by connecting a 220 V-50 Hz source voltage in series with the source inductance $(L_S = 0.1\ mH)$, in parallel with the inductance component $(L_S = 0.1\ mH)$, using a circuit breaker 1 (CB1) with normally open (NO) condition. The system connected to LL is a static load with nominal active power $(P_{SL} = 11\ kW)$ and reactive power $(Q_{SL} = 6\ kVAR)$. CB 4 is ON and CB 5 is OFF.
b. OPM 2 (S-Swell-LL): In OPM 2, the system is connected to LL and the sinusoidal source experiences a 50% swell voltage. The swell voltage is generated by connecting a 220 V-50 Hz source voltage in series with the source inductance component $(L_S = 0.1\ mH)$, in parallel with a 330 V-50 Hz source voltage via a CB 2 with NO condition. The system connected to LL is in the form of a static-nominal load of active power $(P_{SL} = 11\ kW)$ and reactive power $(Q_{SL} = 6\ kVAR)$. CB 4 is ON and CB 5 is OFF.

Table 1. Abbreviation

Symbol	Description
THD	Total Harmonics Distortion
UPQC	Unified Power Quality Conditioner
SeAF	Series Active Filter
ShAF	Shunt Active Filter
LEDSM	Linear Equivalent Discrete System Model
ZVS	Zero Voltage Switching
ZCS	Zero Current Switching
TL-UPQC	Three-Leg UPQC
SOGI-PLL	Second Order Generalized Integrator-Phase Locked Loop
IRPT	Instantaneous Reactive Power Theory
VSI	Voltage Source Inverter
BES	Battery Energy Storage
DG	Distributed Generation
SVPWM	Space Vector Pulse Width Modulation
WE	Wind Energy
MPPT	Maximum Power Point Tracking
ANN	Artificial Neural Networks
STF	Self-Tuning Filter
UVG	Unit Vector Generator
SRF-PLL	Synchronous Reference Frame-Phase Locked Loop
3P3W	Three-Phase Three-Wire
3P4W	Three-Phase Four-Wire
QAB	Quadruple Active Bridge
PV	Photovoltaic
PI	Proportional Integral
FLC	Fuzzy Logic Controller
FIS	Fuzzy Inference System
OPM	Operating Mode
PH	Phase
UVTG	Unit Vector Template Generation
MOSFET	Metal Oxide Semiconductor Field Effect Transistor
IGBT	Insulated Gate Bipolar Transistor

c. OPM 3 (S-Inter-LL): In OPM 3, the system is connected to LL and the sinusoidal source experiences 100% voltage interruption. The interruption voltage is generated by short-circuiting a 220 V-50 Hz source voltage connected in series with the inductance component $(L_S = 0.1\,mH)$, in parallel through CB 3 with NO condition. The system connected to LL is in the form of a static-nominal load of active power $(P_{SL} = 11\,kW)$ and reactive power$(Q_{SL} = 6\,kVAR)$. CB 4 is ON and CB 5 is OFF.

d. OPM 4 (S-Sag-NLL), OPM 4 is the same as OPM 1. The difference is that the system is connected to a NLL in the form of four diodes which function as the switch of four pulses bridge rectifier $(S_1, S_2, S_3, and\ S_4)$ connected to a static load with nominal active $(P_{SL} = 11\,kW)$ and reactive power$(Q_{SL} = 6\,kVAR)$. CB 4 is OFF and CB 5 is ON.

e. OPM 5 (S-Swell-NLL), OPM 5 is the same as OPM 2. The difference is that the system connected to the NLL is a four-pulse bridge rectifier connected to a static load with nominal active $(P_{SL} = 11\,kW)$ and reactive power$(Q_{SL} = 6\,kVAR)$. CB 4 is OFF and CB 5 is ON.

f. OPM 6 (S-Inter-NLL), OPM 6 is the same as OPM 3. The difference is that the system connected to the NLL is a four-pulse bridge rectifier connected to a static load with nominal active power $(P_{SL} = 11\,kW)$ and reactive power$(Q_{SL} = 6\,kVAR)$. CB 4 is OFF and CB 5 is ON.

The total simulation time is $0.5\,sec$ with a disturbance duration of $0.2\,sec$ between $0.15\,sec$ to $t = 0.35\,sec$.

The FLC method is implemented as a DC voltage control on ShAF to improve the power quality of the six OPMs and the results are compared with the PI control. In each OPM, the single-phase UPQC-PV circuits each use PI and FLC controls for a total of 12 OPMs. The results of the analysis were carried out on the parameters, namely the magnitude of the source voltage, the magnitude of the load voltage, the magnitude of the source current, the magnitude of the load current, the THD of the source voltage, the THD of the load voltage, the THD of the source current, the THD of the load current, and the real power of the load. After all these parameters are obtained, the next step is to determine the percentage of load voltage disturbance and load active power on the single-phase UPQC-PV model connected to linear/non-linear loads. The goal is to determine a single-phase UPQC-PV circuit model that is capable of producing the best performance with indicators i.e. lowers source current THD and load voltage THD and maintains load voltage and load active power at six OPM faults. Fig. 1 shows a configuration model of a single-phase UPQC-PV system without a DC link capacitor. Fig. 2 shows the active power flow of a single-phase UPQC-PV configuration without a DC link capacitor. The abbreviations and simulation parameters are shown in Table 1 and Appendix Section respectively.

2.2 Single phase series active filter control

The unit vector templates generation (UVTG) method is used as a serial active filter

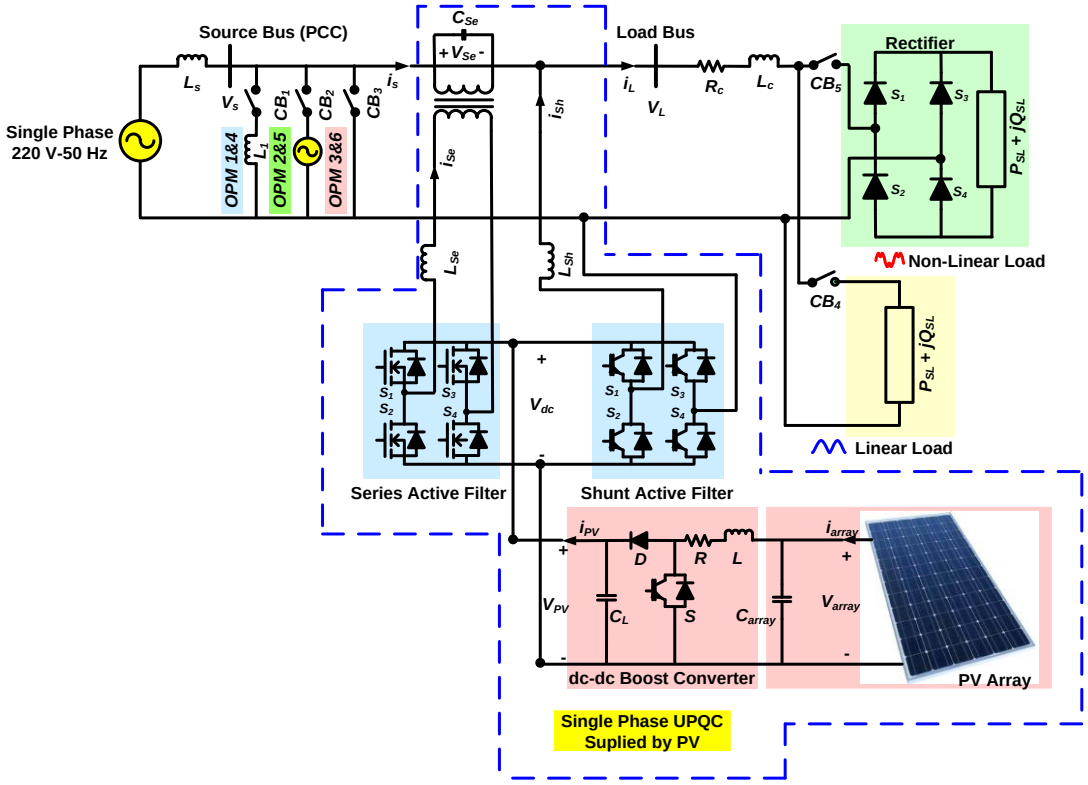

Figure. 1 Proposed model of a single-phase UPQC-PV system without a DC link capacitor

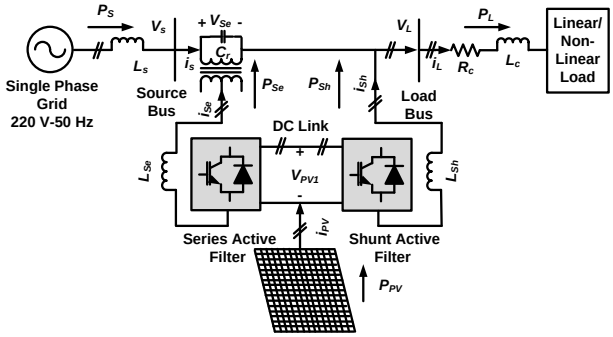

Figure. 2 Active power flow of a single-phase UPQC-PV system without a DC link capacitor

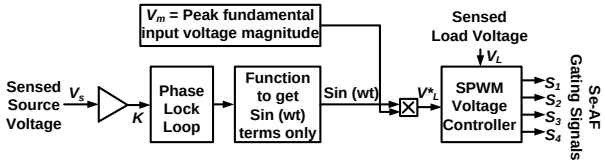

Figure. 3 Series active filter control connected to a single-phase system using the UVTG method

control on a single UPQC connected to a single-phase system [23].

The magnitude value of the peak fundamental input voltage (V_m) is determined at 220 V. The single-phase Se-AF control block is shown in Fig. 3.

2.3 Single phase shunt active filter control

As part of the UPQC control, Sh-AF control in a single-phase system has been fully described in [24]. P-Q theory or power theory at any time, in general, is often used in 3P3W systems and 3P4W systems. This theory uses three voltage and current signals, but can also be applied to single-phase active filters by duplicating two voltage and current signals again with an angle shift of 120º. The basis of this theory is the division of the power components into mean and oscillation. Assign phase "a" to the load current of a single-phase load, and phases "b" and "c" to the additional phases of the doubling technique. Mathematically, the load current can be expressed as the phase current "a" using Eq. (1). If it is assumed that Eq. (1) is the load current for the phase "a", Eq. (2) and Eq. (3) can be used to describe the load current for phases "b" and "c", respectively.

$$i_a = \sum_{i=0}^{n} \sqrt{2}\, I_i \sin(w_i + \theta_i) \quad (1)$$

$$i_b = \sum_{i=0}^{n} \sqrt{2}\, I_i \sin\,(w_i + \theta_i - 120°) \quad (2)$$

$$i_c = \sum_{i=0}^{n} \sqrt{2}\, I_i \sin\,(w_i + \theta_i - 120°) \quad (3)$$

Eq. (1), Eq. (2) and Eq. (3) can be converted into matrices of the form as shown in Eq. (4) and Eq. (5) for load current and load voltage respectively:

$$\begin{bmatrix} i_a \\ i_b \\ i_c \end{bmatrix} = \begin{bmatrix} 1 \\ 1\angle 120° \\ 1\angle 240° \end{bmatrix} [i_a] \tag{4}$$

$$\begin{bmatrix} v_a \\ v_b \\ v_c \end{bmatrix} = \begin{bmatrix} 1 \\ 1\angle 120° \\ 1\angle 240° \end{bmatrix} [v_a] \tag{5}$$

By using Eq. (6) for load current and Eq. (7) for load voltage, the reference current and reference voltage can be calculated using the Clarke transform method as follows:

$$\begin{bmatrix} i_\alpha \\ i_\beta \\ i_o \end{bmatrix} = \sqrt{\frac{2}{3}} \begin{bmatrix} 1 & -\frac{1}{2} & \frac{1}{2} \\ 0 & \frac{\sqrt{3}}{2} & -\frac{\sqrt{3}}{2} \\ \frac{1}{\sqrt{2}} & \frac{1}{\sqrt{2}} & \frac{1}{\sqrt{2}} \end{bmatrix} \begin{bmatrix} i_a \\ i_b \\ i_c \end{bmatrix} \tag{6}$$

$$\begin{bmatrix} v_\alpha \\ v_\beta \\ v_o \end{bmatrix} = \sqrt{\frac{2}{3}} \begin{bmatrix} 1 & -\frac{1}{2} & \frac{1}{2} \\ 0 & \frac{\sqrt{3}}{2} & -\frac{\sqrt{3}}{2} \\ \frac{1}{\sqrt{2}} & \frac{1}{\sqrt{2}} & \frac{1}{\sqrt{2}} \end{bmatrix} \begin{bmatrix} v_a \\ v_b \\ v_c \end{bmatrix} \tag{7}$$

According to [24], active and reactive power are respectively expressed as Eq. (8), Eq. (9), and Eq. (10):

$$p = v_a i_a + v_\beta i + v_o i_o \tag{8}$$

$$q = v_a i_a - v_\beta i_\beta \tag{9}$$

$$\begin{bmatrix} p \\ q \end{bmatrix} = \begin{bmatrix} v_\alpha & v_\beta \\ -v_\beta & v_\alpha \end{bmatrix} \begin{bmatrix} i_\alpha \\ i_\beta \end{bmatrix} \tag{10}$$

The two parts that make up the active power and reactive power are the average and oscillating power, or the DC part and the AC part, respectively. The active power and reactive power are stated in Eq. (11) and Eq. (12) below:

$$p = \bar{p} + \tilde{p} \tag{11}$$

$$q = \bar{q} + \tilde{q} \tag{12}$$

A low-pass filter, which can remove high frequencies and produce a basic component or DC portion, can be used to determine the DC portion. Eq. (13) can be used to describe the reference current α-β from the DC active power and reactive power sections [25].

$$i^*_{\alpha\beta} = \frac{1}{v_\alpha^2 + v_\beta^2} \begin{bmatrix} v_\alpha & v_\beta \\ v_\beta & -v_\alpha \end{bmatrix} \begin{bmatrix} -\tilde{p} + \bar{p}_{loss} \\ -q \end{bmatrix} \tag{13}$$

The average active power is obtained using the $\bar{p}_{loss}$ parameter from the voltage control. This value is in the form of intermittent active power which corresponds to resistive losses and UPQC switching losses. Before the signal is reduced to load current, the three-phase active power filter reference current is given in Eq. (14). A pulse width modulation (PWM) signal is generated using a hysteresis band and reduced three-phase current. Only two of the six PWM signals generated by the hysteresis band are used as hysteresis band inputs for a single Sh-AF.

$$i^*_{abc} = \sqrt{\frac{2}{3}} \begin{bmatrix} 1 & 0 \\ -1/2 & \sqrt{3}/2 \\ -1/2 & -\sqrt{3}/2 \end{bmatrix} i^*_{\alpha\beta} \tag{14}$$

In order to operate properly, a single UPQC must have a minimum DC-link voltage (V_{dc}) which is stated in Eq. (15) [20].

$$V_{dc} = \frac{2\sqrt{2}V_{Ph-N}}{\sqrt{3}m} \tag{15}$$

Using a modulation value (m) of 1 and a phase-to-neutral source voltage V_{Ph-N} of 220 V, the V_{dc} is calculated to equal 359.26 V and set at 400 V.

Based on Eq. (1) to Eq. (14), the authors then develop the FLC control model on the Shunt-AF circuit connected to a single-phase system and the results of which are shown in Fig. 4.

2.4 Fuzzy logic controller design

The FLC method on Shunt-AF on the UPQC-PV circuit begins by determining the UPQC switching losses ($\bar{p}_{loss}$) as input variables, to produce a reference source current on the hysteresis current control and generate a trigger signal on the active shunt IGBT filter circuit from UPQC with PI 1 and PI 2 control ($K_P = 0.2$ and ($K_I = 1.5$). Using the same procedure, $\bar{p}_{loss}$ is also determined using FLC. Each FLC block consists of Fuzzification, decision-making (rulebase, database, reason-mechanism), and defuzzification are shown in Fig. 5. FIS uses the Mamdani method with max-min for both input and output variables. FIS consists of three parts, namely rulebase, database, and reason- mechanism [17].

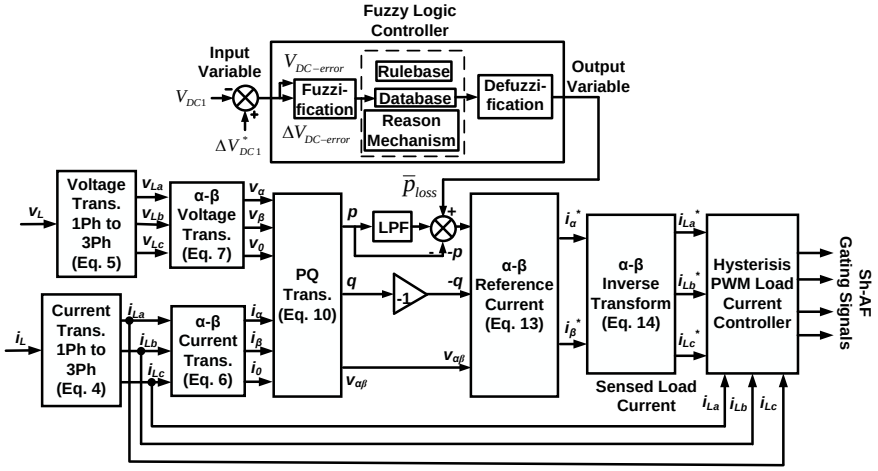

Figure. 4 Active shunt filter control on a single-phase system using the FLC method

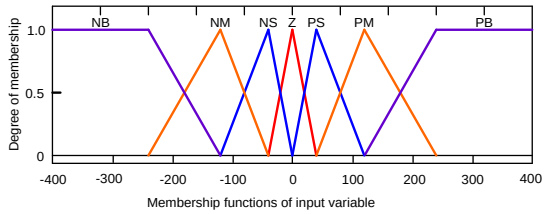

Figure. 5 Input MFs of $V_{DC-error}$

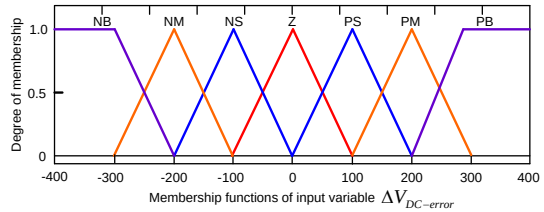

Figure. 6 Input MFs of $\Delta V_{DC-error}$

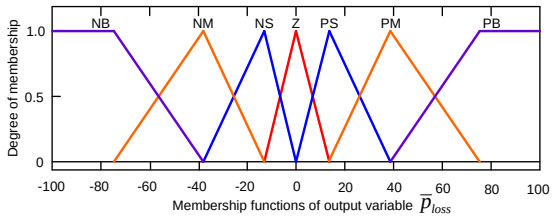

Figure 7. Output MFs of $\bar{p}_{loss}$

Table 2. Fuzzy rule base

a / ***b***	**NB**	**NM**	**NS**	**Z**	**PS**	**PM**	**PB**
PB	Z	PS	PS	PM	PM	PB	PB
PM	NS	Z	PS	PS	PM	PM	PB
PS	NS	NS	Z	PS	PS	PM	PM
Z	NM	NS	NS	Z	PS	PS	PM
NS	NM	NM	NS	NS	Z	PS	PS
NM	NB	NM	NM	NS	NS	Z	PS
NB	NB	NB	NM	NM	NS	NS	Z
$\boldsymbol{a = V_{DC-error}; b = \Delta V_{DC-error}}$							

The FLC method is used to determine the input variables i.e. V_{DC} error ($V_{DC-error}$) and delta V_{DC} error ($\Delta V_{DC-error}$), as well as output variable ($\bar{p}_{loss}$) in the defuzzification phase.

The value of $\bar{p}_{loss}$ is the input variable to obtain the compensating current ($i^*_{\alpha\beta}$) in Eq. (13). During the fuzzification process, several of input variables are calculated and converted into linguistic variables called memberships functions (MFs). The values of two input variables and one output variable on the MFs are divided into seven linguistic variable crips each. The input crips variables used in the seven $V_{DC-error}$ and $\Delta V_{DC-error}$ are NB (negative big), NS (negative medium), NM (negative small), Z (zero), PS (positive small), PM (positive medium) and PB (positive big). The crips of the two input variables are triangular and trapezoidal MF with a limit between -400 and 400. Similar to the input crips variable, the output crips variable is $\bar{p}_{loss}$ in the form of a triangular and trapezoidal but has an MF limit between -100 to 100. The input variable crips and output variables crips each have the same linguistic variables. MF input $V_{DC-error}$, MF input $\Delta V_{DC-error}$, dan MF output $\bar{p}_{loss}$ of FLC are presented in Fig. 5, Fig. 6, and Fig. 7, respectively. After $V_{DC-error}$ and $\Delta V_{DC-error}$ are obtained, the two MF inputs are then converted into linguistic variables and used as input functions for FLC. Table 2 presents the MF output using an inference block with a fuzzy rule base of 49. Furthermore, the defuzzification block finally operates to change the MF output $\bar{p}_{loss}$ resulting from linguistic variables into numerical variables again. The $\bar{p}_{loss}$ value then becomes the input variable to control the hysteresis current to produce a trigger signal to the IGBT at Sh-AF on the UPQC while reducing the source current harmonics. Then at the same time, the UVTG control on Se-AF is in charge of controlling the load voltage to improve the power quality in a single-phase system from six predetermined OPMs.

2.5 Percentage Sag/Swell and Interruption

The monitoring of sag/swell and interruption voltage is validated by IEEE 1159-1995 [26]. This regulation provides a table of definitions of voltage sag/voltage and interruption by category (instantaneous, instantaneous and transient) typical duration, and typical magnitude. The author proposes the percentage of disturbance, namely sag/swell and disturbance voltage in Eq. (16) below. The $V_{pre-distrurb}$ is selected as 220 V.

$$Disturb\ Voltage\ (\%) = \frac{|Vpre\_disturb - V\_disturb|}{Vpre\_disturb} \quad (16)$$

3. Results and discussion

3.1 Simulation result

The proposed model is a UPQC-PV combination connected to a single-phase system (on-grid) via a DC link circuit without capacitors. Two UPQC-PV combinations are proposed, namely, UPQC-PV connected to a LL and UPQC-PV connected to a NLL. Two single-phase CBs (CB 4 and CB 5) are used to connect and disconnect the UPQC-PV circuit in each combination. Fault simulation on single-phase UPQC-PV combinations i.e. OPM 1 (S-Sag-LL), OPM 2 (S-Swell-LL), OPM 3 (S-Inter-LL), OPM 4 (S-Sag-NLL), OPM 5 (S-Swell-NLL), and OPM 6 (S-Inter-NLL). Each UPQC-PV combination uses FLC and is validated by PI control so that a total of 12 OPMs.

By using Matlab Simulink, each model combination is run according to the proposed OPM to obtain the curve for source voltage (V_S) series voltage (V_{SE}), load voltage (V_L), source current (I_S), shunt current (I_{SH}), and load current (I_L). Based on this curve, the magnitude of the source voltage (V_S) series voltage (V_{SE}), load voltage (V_L), source current (I_S), shunt current (I_{SH}), and load current (I_L) is obtained. Furthermore, the values of $THD\ V_S$, $THD\ V_{SE}$, $THD\ V_L$, $THD\ I_S$, $THD\ I_{SH}$, and $THD\ I_L$ are determined based on a number of curves that have been plotted previously. Measurement of the magnitude of the voltage parameter, nominal current, and THD value for each UPQC-PV combination, was carried out in 3 cycles between $t = 0.22\ sec$ to $t = 0.28\ sec$. The next process is to carry out simulations on a number of proposed cases to obtain curves and determine the value of PV voltage (V_{PV}), PV current (I_{PV}), and PV power (P_{PV}) and their contribution to changes in load power (P_L). The PV power value is

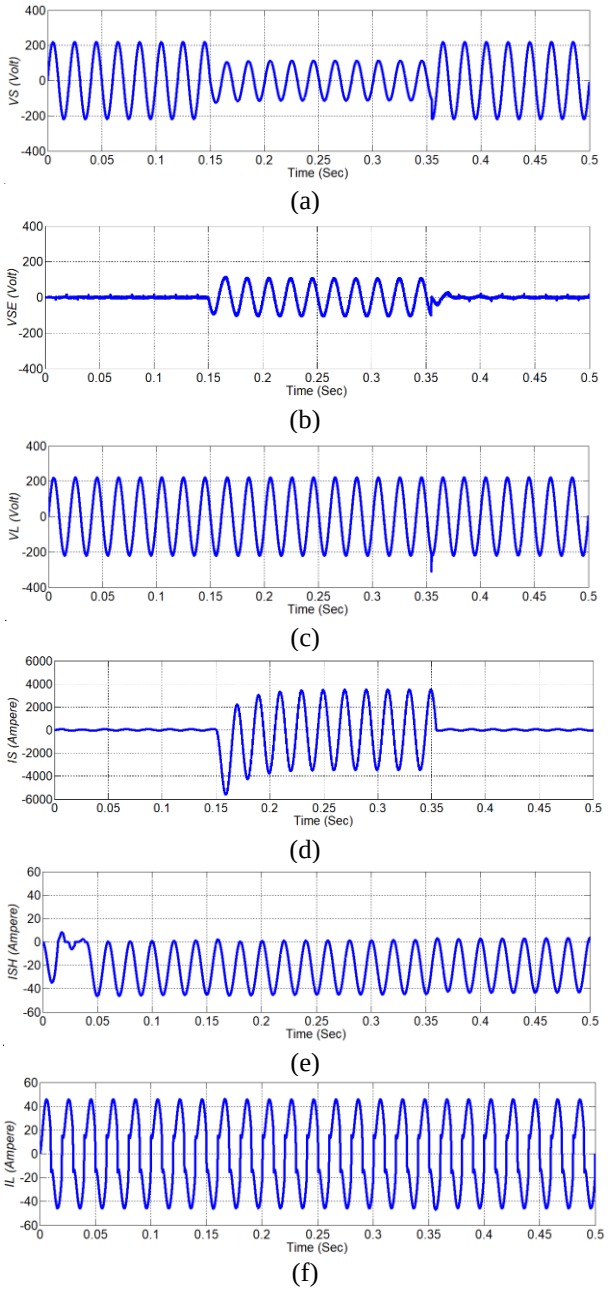

Figure. 8 Performance on single phase UPQC-PV with FLC at OPM 4 (S-Sag-NLL): (a) V_S, (b) V_{SE}, (c) V_L, (d) I_S, (e) I_{SH}, and (f) I_L

the PV output power after the dc-dc boost converter circuit so the value is the same as the DC-link power because the UPQC circuit does not use capacitors. Measurements of PV voltage (V_{PV}), PV current (I_{PV}), PV power (P_{PV}), and load power (P_L) parameters are carried out in one cycle at $t = 0.25\ sec$. The total simulation time for disturbances at OPM 1 to OPM 6 is $t = 0.5\ sec$ with a disturbance duration between $t = 0.15\ sec$ to $t = 0.35\ sec$.

Fig. 8 shows the performance of V_S, V_{SE}, V_L, I_S, I_{SH} and I_L on a single-phase UPQC-PV connected system using FLC at OPM 4 (S-Sag-NLL) conditions.

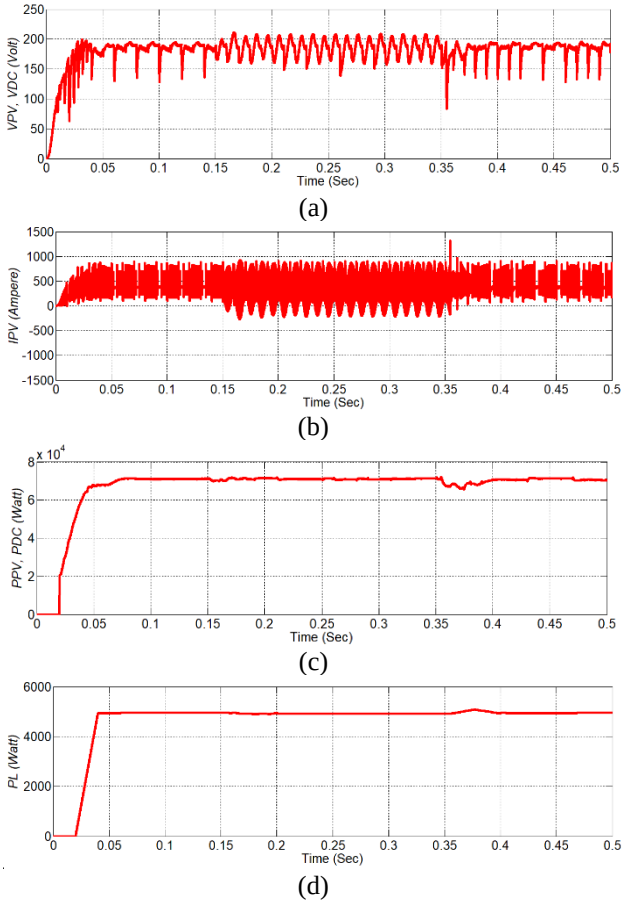

Figure. 9 Performance of single phase UPQC-PV with FLC on OPM 4 (S-Sag-NLL): (a) V_{PV}, V_{DC}, (b) I_{PV}, (c) P_{PV}, P_{DC}, and (d) P_L

Fig. 9 shows the performance of V_{PV}, V_{DC}, I_{PV}, P_{PV}, P_{DC}, and P_L in the same configuration, control, and OPM.

Fig. 8 shows that at t=0.15 sec to t=0.35 sec of the total simulation duration $t = 0.35\ sec$, the source voltage (V_S) drops 50% from 220 V to 113.3 V. In this condition, PV is less able to generate voltage The maximum DC (V_{DC}) and only injects a series compensation voltage (V_{SE}) of 104.7 V through the series transformer on Se-AF. So that in the OPM 4 period, the load voltage (V_L) on a single-phase system slightly decreased by 218 V. The decrease in load voltage (V_L) eventually also caused the load current (I_L) to slightly decrease to 46.10 A. On the other hand, at the same OPM, the single-phase UPQC-PV configuration is capable of injecting a shunt compensating current (I_{SH}) of 23.12 A and a THD of 0.31% in the opposite phase direction so as to reduce the THD of the source current (I_S) to 0.47 % compared to the load current THD (I_L) of 18.48%. In OPM, configuration and control method is the same, Fig. 9 shows that because the system does not use DC-link capacitors, the DC voltage (V_{DC}) is

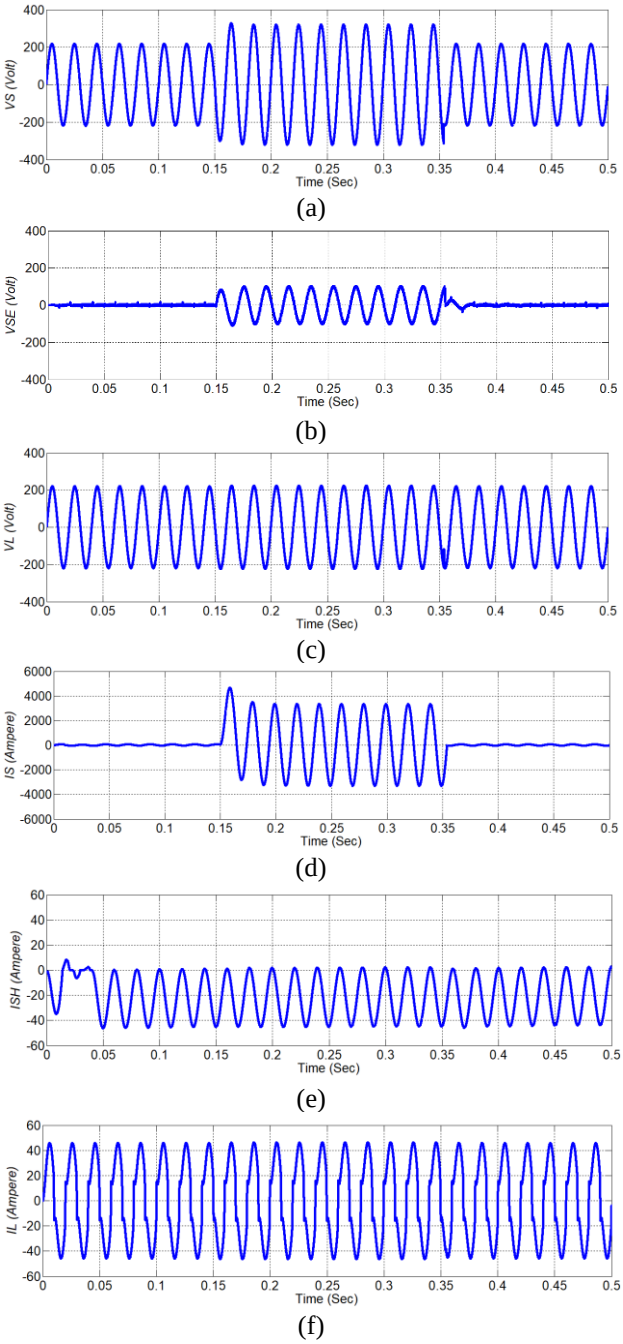

Figure. 10 Performance on single phase UPQC-PV with FLC at OPM 5 (S-Swell-NLL): (a) V_S, (b) V_{SE}, (c) V_L, (d) I_S, (e) I_{SH}, and (f) I_L

the same as the PV voltage (V_{PV}) of 186.4 V. PV generator capable of generating PV output power 〚(P_{PV}) and delivering PV (I_{PV}) output current of 70940 W and 450.8 A respectively. In OPM, the configuration and control methods are the same, Fig. 9 also shows that the value of the PV output power (P_{PV}) equals DC power (P_{DC}) and is capable of delivering 4921 W of (P_L) load power.

Fig. 10 shows the performance of V_S, V_{SE}, V_L, I_S, I_{SH} and I_L on a single-phase UPQC-PV connected

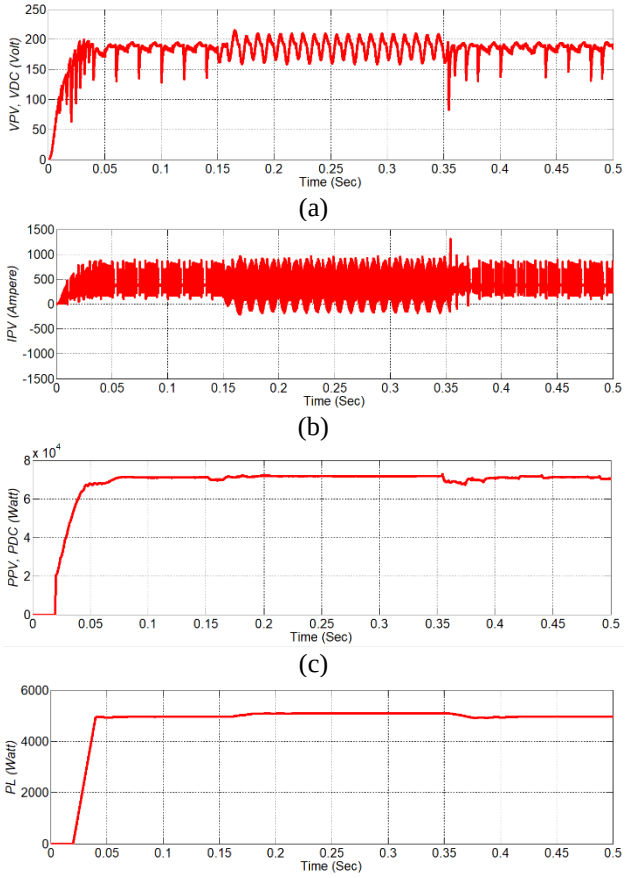

Figure. 11 Performance of V_{PV}, V_{DC}, I_{PV}, P_{PV}, P_{DC} and P_L of single phase UPQC-PV with FLC on OPM 5 (S-Swell-NLL)

system using FLC at OPM 5 (S-Swell-NLL) conditions. Fig. 11 shows the performance of V_{PV} , V_{DC} , I_{PV} , P_{PV} , P_{DC} , and P_L on the same configuration, control, and OPM.

Fig. 10 shows that at $t = 0.15\,sec$ to $t = 0.35\,sec$ of the total duration of the simulation $t = 0.5\,sec$, the source voltage (V_S) increases 50% from 220 V to 320.9 V. In this condition, PV is able to generate DC voltage (V_{DC}) maximum and able to inject series compensated voltage (V_{SE}) with an opposite phase of 99.14 V through series transformer on Se-AF. So that in the OPM 5 period, the load voltage (V_L) on the single-phase system increased slightly by 221.8 V. The increase in load voltage (V_L) eventually also caused the load current (I_L) to slightly increase to 46.87 A. On the other hand, at the same OPM, the single-phase UPQC-PV configuration is capable of injecting a shunt compensating current (I_{SH}) of 23.53 A and a THD of 0.26% in the opposite phase direction so as to reduce the THD of the source current (I_S) to 0.03 % compared to the load current THD (I_L) of 18.79%. At OPM, the configuration and control method is the

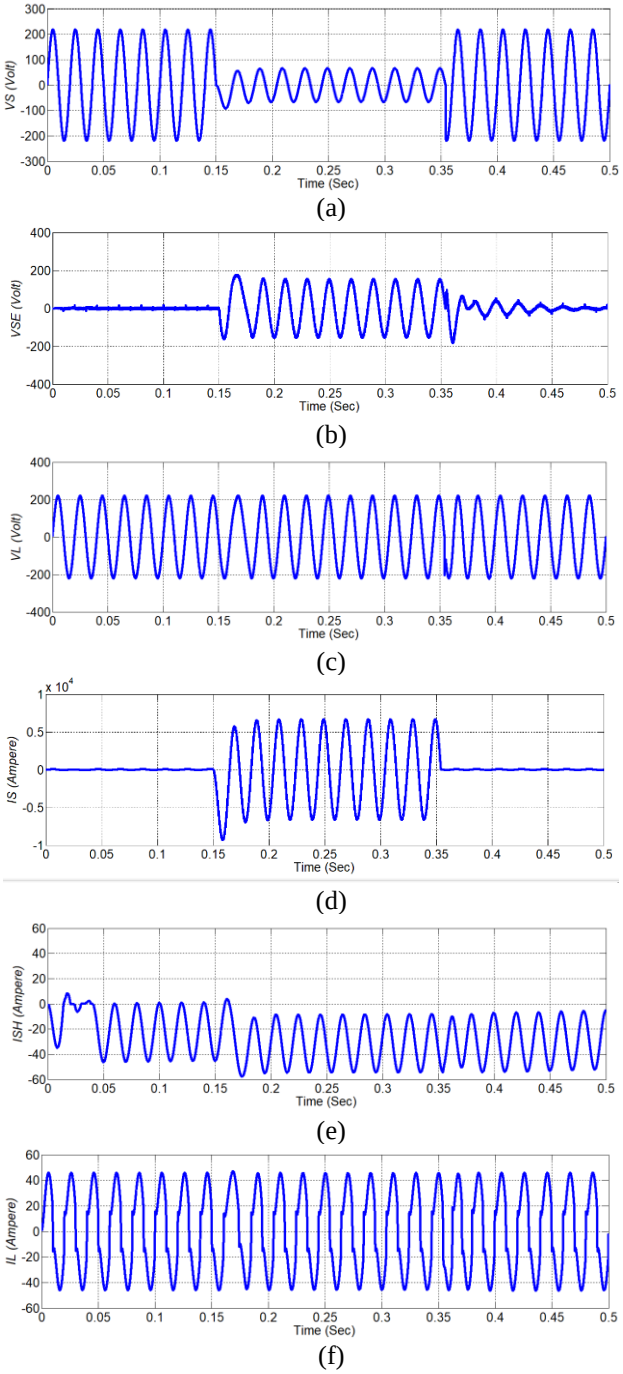

Figure. 12 Performance on single phase UPQC-PV with FLC at OPM 6 (S-Inter-NLL): (a) V_S, (b) V_{SE}, (c) V_L, (d) I_S,(e) I_{SH}, and (f) I_L

same, Fig. 11 shows that because the system does not use DC-link capacitors, the DC voltage (V_{DC}) is the same as the PV voltage (V_{PV}) of 172.8 V. PV generator capable of generating PV output power (P_{PV}) and flowing PV (I_{PV}) output current of 71780 W and 602.6 A, respectively. Fig. 11 also shows that the value of PV output power (P_{PV}) is the same as DC power (P_{DC}) and capable of delivering (P_L) load power of 5088 W.

Table 3. Magnitude of voltage and current using single phase UPQC supplied by PV

OPMs	Source Voltage V_s (V)	Load Voltage V_L (V)	Source Current I_S (A)	Load Current I_L (A)	Series Voltage V_{se} (V)	Shunt Current I_{sh} (A)	Load Voltage Disturb $V_{Disturb}$ (%)
Proportional Integral Controller							
1	113.2	217.9	3486	45.71	104.48	-23.12	0.95
2	320.9	221.8	3321	46.51	99.17	-23.53	0.82
3	66.22	218.3	6661	45.75	152.40	-22.91	0.77
4	113.3	218.0	3483	46.10	104.70	-23.12	0.91
5	320.9	221.8	3320	46.87	99.17	-23.53	0.82
6	66.21	218.3	6664	46.16	152.4	-22.92	0.77
Fuzzy Logic Controller							
1	113.2	217.9	3486	45.71	104.7	-23.12	0.95
2	320.9	221.8	3321	46.51	99.14	-23.53	0.82
3	66.22	218.5	6661	45.79	152.6	-22.89	0.68
4	113.3	218.0	3483	46.10	104.7	-23.12	0.91
5	320.9	221.8	3320	46.87	99.14	-23.53	0.82
6	66.21	218.5	6664	46.20	152.6	-22.90	0.68

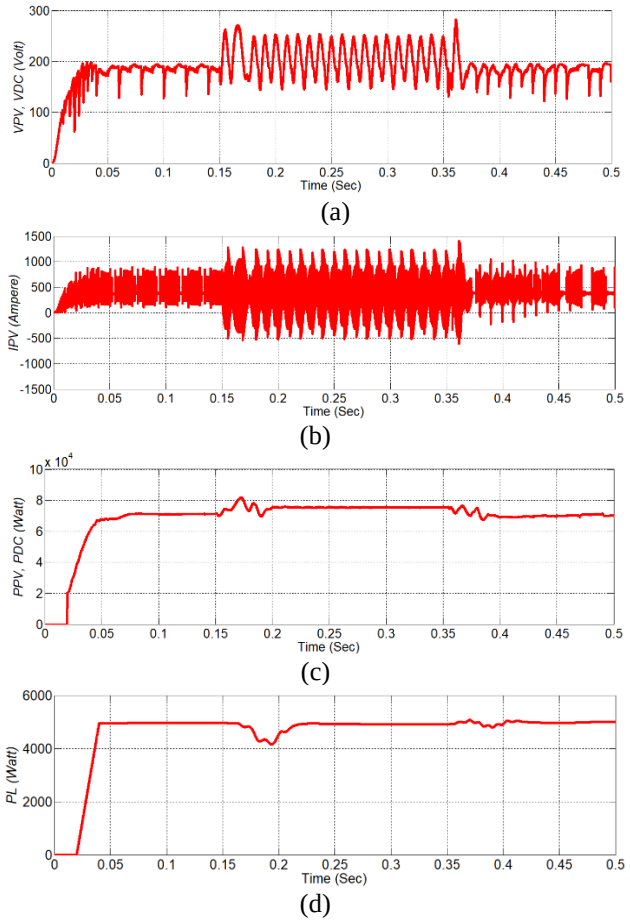

Figure. 13 Performance of V_{PV}, V_{DC}, I_{PV}, P_{PV}, P_{DC} and P_L of single phase UPQC-PV with FLC on OPM 6 (S-Inter-NLL)

Fig. 12 shows the performance of V_S, V_{SE}, V_L, I_S, I_{SH} and I_L on a UPQC-PV connected single-phase system using FLC at OPM 6 (S-Inter-NLL). Fig. 13 shows the performance of V_{PV}, V_{DC}, I_{PV}, P_{PV}, P_{DC}, and P_L on the same configuration, control, and OPM.

Fig. 12 shows that $t = 0.15\ sec$to $t = 0.35\ sec$ of the total duration of the simulation $t = 0.5\ sec$, the source voltage (V_S) drops from 220 V to 66.21 V. In this condition, the PV is able to maintain the DC voltage (V_{DC}) and is able to inject series compensated voltage (V_{SE}) with an opposite phase of 152.6 V through a series transformer on Se-AF. So that in the OPM 6 period, the load voltage (V_L) on a single-phase system slightly decreased by 218.5 V. The decrease in load voltage (V_L)) eventually also caused the load current (I_L) to slightly decrease to 46.20 A. On the other hand, at the same OPM, the single-phase UPQC-PV configuration is capable of injecting a shunt compensating current (I_{SH}) of 22.99 A and a THD of 3.07% in the opposite phase direction so as to reduce the THD of the source current (I_S) to 0.01 % compared to the load current THD (I_L) of 18.36%. In OPM, the configuration and control method is the same, Fig. 13 shows that because the system does not use DC-link capacitors, the DC voltage (V_{DC}) is the same as the PV voltage (V_{PV}) of 249.8 V. PV generator capable of generating PV output power (P_{PV}) and flowing PV output current (I_{PV})of 75580 W and 363.6 A, respectively. Fig. 13 also shows that the value of PV output power (P_{PV}) is the same as DC power (P_{DC}) and capable of delivering load power (P_L) of 5928 W.

Using the same procedure, all parameter values V_S, V_{SE}, V_L, I_S, I_{SH}, I_L, $V_{Disturb}$ and THD values are presented in Table 3 and Table 4 respectively. The values of V_{PV}, V_{DC}, I_{PV}, P_{PV}, P_{DC} and P_L in The different OPM and single-phase UPQC-PV configurations respectively using the PI and FS control methods are fully presented in full in Table 5.

Table 4. Voltage and current THD using single phase UPQC supplied by PV

OPMs	THD Source Voltage V_s (V)	THD Load Voltage V_L (V)	THD Source Current I_S (A)	THD Load Current I_L (A)	THD Series Voltage V_{se} (V)	THD Shunt Current I_{sh} (A)
Proportional Integral Controller						
1	0.16	0.98	1.07	0.52	3.27	0.51
2	0.01	0.84	0.09	0.40	3.52	0.34
3	0.10	3.55	0.08	3.38	5.36	4.52
4	1.05	0.99	1.07	18.48	3.39	0.49
5	0.03	0.86	0.09	18.78	3.56	0.37
6	0.15	3.56	0.08	18.56	5.37	4.46
Fuzzy Logic Controller						
1	0.07	0.90	0.47	0.34	3.20	0.32
2	0.00	0.79	0.02	0.28	3.46	0.23
3	0.03	2.14	0.01	1.92	3.50	3.12
4	1.02	0.90	0.47	18.48	3.31	0.31
5	0.03	0.81	0.03	18.79	3.53	0.26
6	0.13	2.15	0.01	18.36	3.50	3.07

Table 5. PV output and load power using single phase UPQC supplied by PV

OPMs	PV Voltage V_{PV} (V)	DC Voltage V_{DC} (V)	PV Current I_{PV} (A)	PV Power P_{PV} (W)	DC Power P_{DC} (W)	Load Power P_L (W)
Proportional Integral Controller						
1	186.2	186.2	446.3	71830	71830	4592
2	174.4	174.4	368.8	71620	71620	4751
3	248.3	248.3	227.6	75690	75690	4589
4	186.4	186.4	450.8	70940	70940	4921
5	172.8	172.8	602.6	71780	71780	5088
6	249.0	249.0	363.0	75880	75880	4928
Fuzzy Logic Controller						
1	186.2	186.2	446.3	71840	71840	4592
2	172.4	172.4	368.4	71620	71620	4751
3	248.3	248.3	227.6	75690	75690	4589
4	186.4	186.4	450.8	70940	70940	4921
5	172.8	172.8	602.6	71780	71780	5088
6	249.0	249.0	363.6	75580	75580	4928

Table 3 shows that at OPM 1 to OPM 6, a single-phase system using a single-phase UPQC-PV with PI control is still able to maintain a load voltage (V_L) between 217.9 to 218.3 V. In the same configuration and using FLC, OPM 1 to OPM 6 disturbances are able to maintain a slightly larger load voltage (V_L) between 217.9 V to 218.3 V. Table 3 also shows that in OPM 1 to OPM 6, a single-phase system uses a single phase UPQC-PV with PI control is capable of flowing load current (I_L) between 45.71 A to 46.87 A. In the same configuration and using FLC, OPM 1 to OPM 6 disturbances are able to carry a slightly larger load current (I_L) each between 45.71 A to 46.87 A. Table 3 also shows that at OPM 1 up to OPM 6, a single phase system using UPQC-PV with PI control produces a change in load voltage ($V_{Disturb}$) between 0.77% to 0.95%. In the same configuration and using FLC, OPM 1 to OPM 6 disturbances are capable of producing low load voltage changes ($V_{Disturb}$) between 0.68% to 0.95%.

Fig. 14 shows that at OPM 4, the single-phase UPQC-PV configuration with FLC is capable of producing a source current THD (I_S) of 0.47%, lower than a load current THD (I_L) of 18.48%. The UPQC-PV configuration with FLC is capable of injecting shunt compensating current (I_{SH}) so that it can significantly reduce the source current THD (I_S) according to IEEE 519 Standard. Fig. 15 shows that in OPM 4, the UPQC-PV configuration with FLC is able to produce THD of the load voltage is 0.90%, lower than the THD of the source voltage of 1.02%. The THD value of load voltage (V_L) is relatively still slightly lower than the THD of the source voltage (V_S) and the component values both meet the voltage THD limit according to the IEEE-519 Standard.

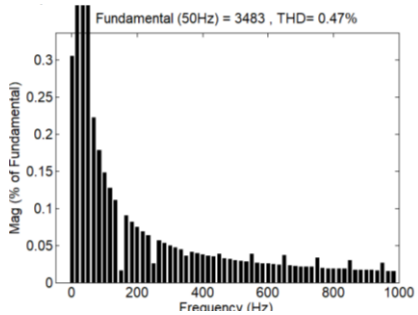

(a)

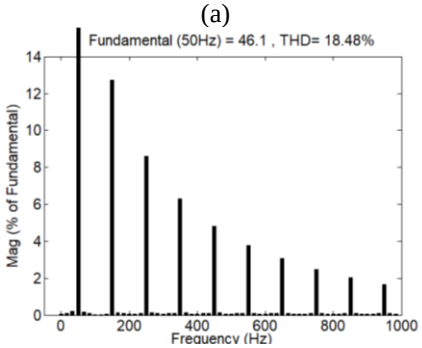

(b)

Figure. 14 Harmonic spectra: (a) I_S and (b) I_L at OPM 4 (S-Sag-NLL) using single-phase UPQC-PV with FLC

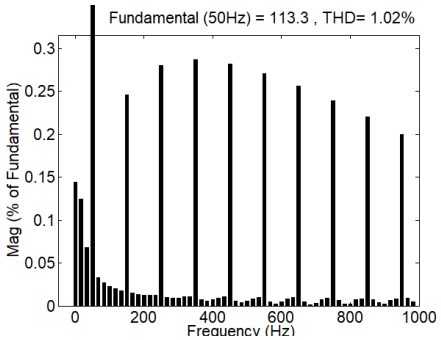

(a)

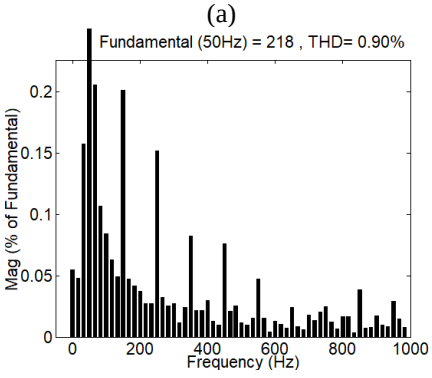

(b)

Figure. 15 Harmonic spectra: (a) V_S and (b) V_L at OPM 4 (S-Sag-NLL) using single-phase UPQC-PV with FLC

In the same procedure, the values of THD V_S,THD V_{SE}, THD V_L, THD I_S,THD I_{SH} and THD I_L in the single-phase UPQC-PV configuration with OPM and different controls were obtained and the results are presented in Table 4.

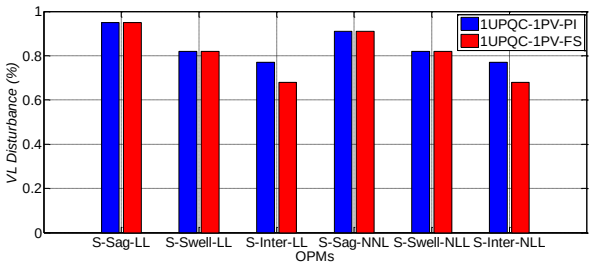

Figure. 16 Performance of load voltage change ($V_{Disturb}$) under six OPMs

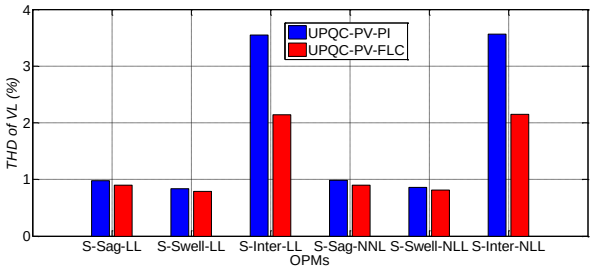

Figure. 17 Performance of load voltage harmonics (V_L)) under six OPMs

Table 4 shows that a single UPQC-PV system with PI control that experiences OPM 1 to OPM 6 disturbances is capable of producing a load voltage THD (V_L) between 0.84% to 3.56%. In the same configuration but using FLC, OPM 1 to OPM 6 interference can reduce the load voltage THD (V_L) to between 0.79% to 2.15%. Table 4 shows that the UPQC-PV system with PI control that experiences interference with OPM 1 to OPM 6 is capable of producing a source current THD (I_S) between 0.08% and 1.07%. In the same configuration but using FLC, OPM 1 to OPM 6 interference can reduce the source current THD (I_S) between 0.01% to 0.47%.

Table 5 shows that the single-phase UPQC-PV combination using PI and FLC is capable of producing the same PV (V_{PV}) and DC voltage (V_{DC}). The PV current (I_{PV}) flowing into the DC-link circuit without a capacitor in the single-phase UPQC-PV combination, then causes the PV (P_{PV}) and DC power (P_{DC}) to be the same value. The OPM 3 and OPM 6 disturbances, in the combination of single-phase UPQC-PV with PI and FS control, show that the PV is able to inject the largest power (P_{PV}) so that it is still able to distribute the load active power (P_L) with a value close to the same with OPM 1, OPM 2, OPM 4, and OPM 5 disturbances.

Fig. 16 shows that in a single-phase system using a single-phase UPQC-PV configuration with PI and FLC control, OPM 1 disturbance is able to produce a maximum voltage change ($V_{Disturb}$) of 0.95%. In the same configuration, the OPM 6 disturbance with FLC is able to result in the lowest load voltage change

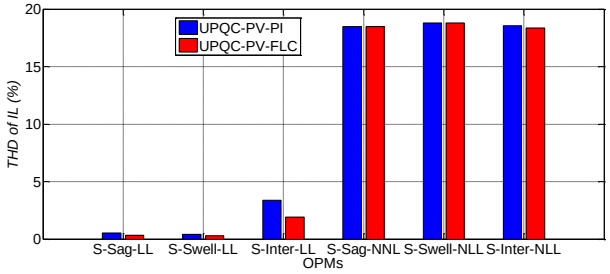

Figure. 18 Performance of load current harmonics (I_L) under six OPMs

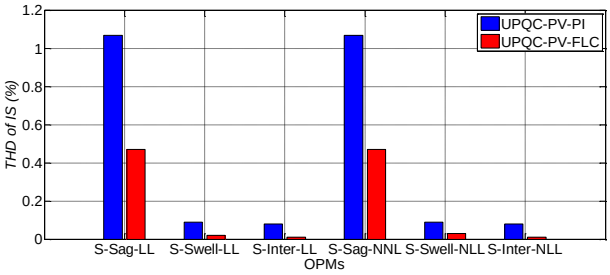

Figure. 19 Performance of source current harmonics (I_S) under six OPMs

($V_{Disturb}$) as 0.68%. The equation is that the change in load voltage in the single-phase UPQC-PV configuration with two different methods and six OPMs is still within the maximum voltage change limit ($V_{Disturb}$ below 5%).

Fig. 17 shows that the OPM 3 and OPM 6 faults in a single-phase UPQC-PV configuration with PI/FLC control are capable of producing the highest load voltage THD ($THD\ V_L$ above 2.14%) compared to other OPMs. OPM 2 and OPM 5 disturbance in single phase UPQC-PV configuration with PI/FLC control is capable of producing the lowest load voltage THD ($THD\ V_L$ above 0.79%) compared to other OPMs. In a single-phase UPQC-PV configuration with OPM 1 to OPM 6 disturbances, FLC is able to produce a lower THD load voltage than the PI control. The system uses a single-phase UPQC-PV which is disturbed by OPM 1 to OPM 6 with PI/FLC control capable of producing a load voltage THD below the IEEE 519 limit.

Fig. 18 shows that the UPQC-PV system with PI/FLC control which experiences OPM 4, OPM 5, and OPM 6 disturbances produce a much higher load current THD (THD above 18.48%) compared to the same combination and control with OPM 1 disturbance, OPM 2, and OPM 3 (THD above 0.28%). However, as shown in Fig. 19, the single-phase UPQC-PV combination for all OPM faults with PI/FLC control is able to inject shunt compensation current (I_L) to the load bus so that it can lower the source current THD (I_S) significantly

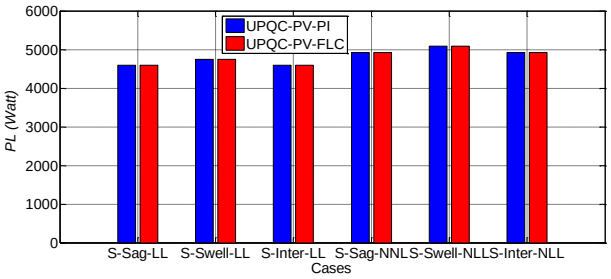

Figure. 20 Performance of load active power (P_L) under six OPMs

lower than the load current THD (I_L) according to IEEE-519. Fig. 19 also explains that in a single-phase UPQC-PV configuration with OPM 1 to OPM 6 faults, FLC is able to produce a source current THD load (I_S) lower than the PI control.

Fig. 20 shows that the UPQC-PV system with PI and FLC control which is experiencing OPM 1 to OPM 6 disturbances, absorbs load active power which has the same value at each OPM. The difference is that the UPQC-PV system with the same control, which experiences OPM 4, OPM 5, and OPM 6 disturbances (P_L above 4921 W) is able to absorb greater load active power than systems which experience OPM 1, OPM 2, and OPM 3 disturbances. (P_L above 4589 W). Thus, the system connected to an NLL is able to absorb a larger active load power in case the source experiences sag/swell and interruption voltage.

3.2. System validation and comparison

Table 6 shows the system validation of the results for the proposed study compared to the six previous studies. The parameters observed are THD of load voltage (V_L), THD of source current (I_S), type of disturbance mitigation, the existence of UPQC injected by PV and battery energy storage (BES). S.A.O. da Silva, et. al, 2017 [9] proposed a 1PH-3PH-UPQC topology in a 3P4W distribution system for remote areas. The types of interference mitigated are sag and NLL resulting in minimum THD V_L and THD I_S values of 1.46% (average) and 4.3%, respectively. The UPQC system uses DC-link capacitors without PV injection and BES. In [10], L.B.G. Champanhol, et. al observed the size, stability analysis and power flow of the 3PH-UPQC-PV system. The type of disturbance that is mitigated is only NLL which produces a minimum THD V_L of 1.8% (average). The UPQC system uses DC-link capacitors and PV injection without BES. L. Meng, et.al [12] have investigated 1PH-UPQC using notch filters and feedback to suppress DC-link voltage ripple due to low-frequency effects. The type of interference that is mitigated is only NLL which

Table 21. Comparison of single phase UPQC-PV without DC-link capacitor using FLC (proposed study) and previous

No.	Authors	Method	THD V_L (V)	THD I_S (A)	Disturbance Mitigation	UPQC Injected by PV	DC Link Capacitor	BES
1.	S.A.O. da Silva, et. al, 2017 [9]	1PH-3PH-UPQC	1.467% (Average)	4.3%	Sag, NLL	NA	A	NA
2.	L.B.G. Campanhol, et. al, 2018 [10]	3PH-UPQC-PV	1.8% (Average)	NA	NLL	A	A	NA
3.	L. Meng, et. al, 2021 [12]	1PH-UPQC-Low Frequency DC-Link Riple	NA	1.32%	NLL	NA	A	NA
4.	K. Sarita, et, al, 2000 [19]	3PH-UPQC-PV-WE- EVA-FLC	6.27% (Average)	2.37% (Average)	Sag, Swell, LL, NLL	A and also with Wind Energy (WE)	A	A
5.	M.A. Mansoor, et, al, 2000 [20]	3PH-UPQC-PV-BES	0.28% (Average)	2.663% (Average)	Sag, Swell, NLL	A	A	A
6.	G. M. Pelz, et. al., 2000 [21]	DG-UPQC-1PH-3PH	1.167% (Average)	2.2%	NLL	A	A	NA
7.	**Proposed Study**	**1PH-UPQC-PV-FLC**	**0.79%**	**0.01%**	**Sag, Swell, Interruption,LL, NLL**	**A**	**NA**	**NA**

Note: A = Available; NA = not available

produces a minimum THD I_S of 1.32%. The UPQC system uses DC-link capacitors without PV injection and BES.

K. Sarita, et.al [19] have observed an increase in power quality using 3PH-UPQC-PV-WE-EVA-FLC which has been observed in depth. The types of interference mitigated are Sag, Swell, LL, and NLL resulting in a minimum THD V_L and THD I_S of 6.27% (average) and 2.37% (average) respectively. The UPQC system uses DC-link capacitors, PV-WE injection, and BES. M.A. Mansor, et. al [20] have investigated power quality problems in grid systems and harmonics due to NLL using 3PH-UPQC-PV-BES. The types of interference mitigated are Sag, Swell, and NLL resulting in a minimum THD V_L and THD I_S of 0.28% (average) and 2.663% (average) respectively. The UPQC system uses a DC-link capacitor, PV-WE injection, and BES. G.M. Pelz, et.al [21] have implemented a DG-UPQC-1PH-3PH) system using PV to serve local loads connected to a 3P3W system, and serving rural and/or remote area customers supplied by a single-phase network. The type of disturbance that is mitigated is only NLL resulting in a minimum THD V_L and THD I_S of 1.67% (average) and 2.2% (average) respectively. The UPQC system uses DC-link capacitors and PV injection.

The authors have observed the 1PH-UPQC-PV-FLC system for mitigating power quality on the source and load sides. The types of disturbances mitigated are Sag, Swell, Interruption, LL, and NLL resulting in a minimum THD V_L and THD I_S of 0.79% and 0.01%, respectively (see Table 4). The THD V_L value of the proposed system is slightly higher than [20], but the THD I_S value is already lower than [12], and both meet the IEEE-519 limits. The system provides the best performance because it is also able to mitigate disturbances to interruption voltage, compared to [19, 20]. The UPQC system also has better circuit efficiency because it only uses PV injection without a DC-link capacitor and BES compared to [19, 20].

4. Conclusion

A single-phase UPQC model integrated with PV using FLC with the Mamdani FIS algorithm connected to a 220V-50 Hz single-phase distribution network has been proposed. Single-phase UPQC-PVs are connected at LL and NLL respectively. The proposed single-phase UPQC design is without using a DC link capacitor circuit. The PV generator system is then used as a DC voltage source which functions to supply load power when the source is interrupted and simultaneously replaces the role of the DC link capacitor circuit to keep the PV output voltage and also the DC link connected to UPQC so that the value remains constant. FLC is used to overcome the weakness of the PI control method in determining the optimum parameters of the proportional constant (K_P) and integral constant (K_I). Fault simulation on a single-phase UPQC-PV combination consisting of six OPMs. In the single-phase UPQC configuration, OPM 6 disturbance with FLC control is able to produce a voltage change $(V_{Disturb})$ as low as 0.68%.

In the same configuration as the OPM 1 to OPM 6 disturbance, the FLC is able to produce a lower load voltage THD and source current THD than the PI control, and has complied with IEEE-519 limits. In the same configuration as PI/FLC control, OPM 4, OPM 5, and OPM 6 disturbances are able to absorb greater load active power than systems with OPM 1, OPM 2, and OPM 3 disturbances.

In the OPM 3 and OPM 6 disturbances during the duration of the disturbance $t = 0.15\ sec$ hingga $t = 0.35\ sec$ the source voltage is still above the limit of the IEEE Standard 1159-1995 interruption voltage of 0.1 p.u [26]. This condition arises because the PV still injects voltage through SeAF and the series transformer even though the source voltage has been zeroed out by short-circuiting. The use of series voltage intelligent control on SeAF can be proposed as future work to solve this problem.

Conflicts of interest

The authors declare no conflict of interest

Author contributions

Conceptualization, Amirullah Amirullah and Adiananda Adiananda; methodology, Amirullah Amirullah and Adiananda Adiananda; software, Amirullah Amirullah; validation, Amirullah Amirullah; formal analysis, Amirullah Amirullah and Adiananda Adiananda; investigation, Amirullah Amirullah and Adiananda Adiananda; resources, Amirullah Amirullah; data curation, Amirullah Amirullah; writing—original draft preparation, Amirullah Amirullah; writing—review and editing, Amirullah Amirullah and Adiananda Adiananda; visualization, Adiananda Adiananda; supervision, Amirullah Amirullah; project administration, Amirullah Amirullah; funding acquisition, Amirullah Amirullah. All authors have read and approved the final manuscript.

Acknowledgments

This work was supported by the Directorate of Research, Technology and Community Service-Ministry of Education, Culture, Research, and Technology, the Republic of Indonesia in the scheme of National Competitive-Fundamental Research 1st year [Decree Letter Number 033/E5/PG.02.00/2022 on 27 April 2022 and Agreement/Contract Number Master Contact Number 159/E5/P6.02.00.PT/2022 on 10 May 2022 and Derivative Contract Number 009/SP2H/PT/LL7/2022 on 10 Mei 2022 and Number 001/VI/2022/LPPM/UBHARA on 10 May 2022]

References

[1] B. Han, B. Hae, H. Kim, and S. Back, "Combined Operation of Unified Power Quality Conditioner with Distributed Generation", *IEEE Transactions on Power Delivery*, Vol. 21, No. 1, pp. 330-338, 2006.

[2] V. Khadkikar, "Enhancing Electric Power Quality UPQC: A Comprehensive Overview", *IEEE Transactions on Power Electronics*, Vol. 27, No. 5, pp. 2284-229, 2012,

[3] Y. Rong, C. Li, H. Tang, and X. Zheng, "Output Feedback Control of Single-Phase, UPQC Based on a Novel Model", *IEEE Transaction on Power Delivery*, Vol. 24, No. 3, pp. 1586-1487, 2009.

[4] K. H. Kwan, P. L. So, and D. Y. C. Chu, "An Output Regulation-Based Unified Power Quality Conditioner with Kalman Filters", *IEEE Transactions on Industrial Electronics*, Vol. 59, No. 11, pp. 4248-4262, 2012.

[5] M. C. Jiang, K. Y. Lu, B. J. Shih, and T. C. Liu, "A Soft-Switching Single-Phase Unified Power Quality Conditioner", In: *Proc. of International Power Electronics Conference*, Hiroshima, Japan, pp. 105-109, 2014.

[6] Y. Lu, G. Xiao, X. Wang, F. Blaabjerg, and D. Lu, "Control Strategy for Single-phase Transformerless Three-Leg Unified Power Quality Conditioner Based on Space Vector Modulation", *IEEE Transactions on Power Electronics*, Vol. 31, No. 4, pp. 2840–2849, 2016.

[7] H. K. Yada and M. S. R. Murthy, "Operation and Control of Single-Phase UPQC based on SOGI-PLL", In: *Proc. of International Conference on Power Electronics*, Patiala, India, pp. 1-6, 2016.

[8] P. V. Kumar and R. Rajeswari, "Adaptive Voltage Detection Controlled Based Single Phase UPQC", In: *Proc. of International Conference on Intelligent Systems and Control*, Coimbatore, India, pp. 1-5, 2016.

[9] S. A. O. D. Silva and F. A. Negrao, "Single-Phase to Three-Phase Unified Power Quality Conditioner Applied in Single-Wire Earth Return Electric Power Distribution Grids", *IEEE Transactions on Power Electronics*, Vol. 33, No. 5, pp. 1-12, 2018.

[10] L. B. G. Campanhol, S. A. O. D. Silva, A. A. D. Oliveira, and V. D. Bacon, "Power Flow and Stability, Analyses of a Multifunctional Distributed Generation System Integrating a Photovoltaic System with Unified Power Quality Conditioner", *IEEE Transactions on*

Power Electronics, Vol. 34, No. 7, pp. 1-16, 2019.

[11] M. R. Soukhtekouhi, M. Hamzeh, and H. I. Eini, "Performance Improvement of Unified Power Quality Conditioner Under Various Load, Source, and Line Conditions Using A New Control Method", In: *Proc. of Power Electronics, Drive Systems, and Technologies Conference*, Tehran, Iran, pp. 1-6, 2020.

[12] L. Meng, L. Ma, W. Zhu, H. Yan, T. Wang, W. Mao, X. He, and Z. Shu, "Control Strategy of Single-Phase UPQC for Suppressing the Influences of Low-Frequency DC-Link Voltage Ripple", *IEEE Transactions on Power Electronics*, Vol. 37, No. 2, pp. 1-12, 2021.

[13] Amirullah, O. Penangsang, and A. Soeprijanto, "High Performance of Unified Power Quality Conditioner and Battery Energy Storage Supplied by Photovoltaic Using Artificial Intelligent Controller", *International Review on Modelling and Simulations*, Vol. 11, No. 4, pp. 221-234, 2018.

[14] Amirullah, O. Penangsang, and A. Soeprijanto, "Matlab/Simulink Simulation of Unified Power Quality Conditioner-Battery Energy Storage System Supplied by PVWind Hybrid using Fuzzy Logic Controller", *International Journal of Electrical and Computer Engineering*, Vol. 9, No. 3, pp. 1479-1495, 2019,

[15] T. M. T. Thentral, K. Vijayakumar, S. Usha, A. Geetha, and D. D. Agarwal, "New Space Vector Pulse Width Modulated Transformer Less Single-Phase Unified Power Quality Conditioner", *Materials Today: Proceedings*, Vol. 45, No. 2, pp. 1750 -1756, 2021.

[16] Amirullah, Adiananda, O. Penangsang, and A. Soeprijanto, "Power Transfer Analysis Using UPQC-PV System Under Sag and Interruption With Variable Irradiance", In: *Proc. of International Conference on Smart Technology and Applications*, Surabaya, Indonesia, pp. 1-7, 2020.

[17] A. Amirullah, A. Adiananda, O. Penangsang, and A. Soeprijanto, "Load Active Power Transfer Enhancement Using UPQC-PV-BES System With Fuzzy Logic Controller", *International Journal of Intelligent Engineering and Systems*, Vol. 13, No. 2, pp. 329-349, 2020, doi: 10.22266/ijies2020.0430.32.

[18] T. Jin, Y. Chen, J. Guo, M. Wang, and M. A. Mohamed, "An Effective Compensation Control Strategy for Power Quality Enhancement of Unified Power Quality Conditioner", *Energy Reports*, Vol. 6, pp. 2167–2179, 2020.

[19] K. Sarita, S. Kumar, A. A. S. Vardhan, R. M. Elavarasan, R. K. Saket, G. M. Shafiullah, and E. Hossain, "Power Enhancement With Grid Stabilization of Renewable Energy-Based Generation System Using UPQC-FLC-EVA Technique", *IEEE Access*, Vol. 3, pp. 207443-207464, 2020.

[20] M. A. Mansor, K. Hasan, M. M. Othman, S. Z. B. M. Noor, and I. Musirin, "Construction and Performance Investigation of Three-Phase Solar PV and Battery Energy Storage System Integrated UPQC", *IEEE Access*, Vol. 8, pp. 1-29, 2020.

[21] G. M. Pelz, S. A. O. D. Silva, and L. P. Sampaio, "Distributed Generation Integrating a Photovoltaic-Based System with a Single-to Three-Phase UPQC Applied to Rural or Remote Areas Supplied by Single-Phase Electrical Power", *Electrical Power and Energy Systems*, Vol. 117, No. 105673, pp. 1-15, 2020.

[22] J. Han, X. Li, Y. Jiang, and S. Gong, "Three-Phase UPQC Topology Based on Quadruple-Active-Bridge", *IEEE Access*, Vol. 9, pp. 4049-5058, 2021.

[23] Y. A. Setiawan and A. Amirullah, "Implementation of Single-Phase DVR-BES Based on Unit Vector Template Generation (UVTG) to Mitigate Voltage Sag Using Arduino Uno and Monitored in Real-Time Through LabVIEW Simulation", *International Journal of Intelligent Engineering and Systems*, Vol. 14, No. 3, pp. 82-96, 2021, doi: 10.22266/ijies2021.0630.08.

[24] M. Y. Lada, O. Mohindo, A. Khamis, J. M. Lazi, and I. W. Jamaludin, "Simulation Single Phase Shunt Active Filter Based on p-q Technique using MATLAB/Simulink Development Tools Environment", In: *Proc. of IEEE Applied Power Electronics Colloquium*, Johor Bahru, Malaysia, pp. 159-164, 2011.

[25] M. Hembram and A. K. Tudu, "Mitigation of Power Quality Problems using Unified Power Quality Conditioner (UPQC)", In: *Proc. of Third International Conference on Computer, Communication, Control, and Information Technology*, pp. 1-5, Hooghly, India, 2015.

[26] *IEEE Std. 1159-1995, IEEE Recommended Practice for Monitoring Electric Power Quality*, The Institute of Electrical and Electronics Engineers, Inc., Piscataway, New York, N.Y. 1995.

Appendix

Parameters of the single-phase UPQC-PV system.

Single phase Grid: RMS voltage (line-neutral) $220\,Volt$, frequency $50\,Hz$, line inductance $L_S = 0.1\,mH$; sag voltage fault generation (OPM 1 and OPM 4): sag parallel inductance $L_1 = 0.1\,mH$, CB_1 breaker resistance $R_{on} = 0.01\,Ohm$, snubber resistance $R_s = 1 \times 10^6\,Ohm$, snubber capacitance $C_s = infinite$, and switching time = [0.15 sec 0.35 sec] with NO condition; swell voltage fault generation (OPM 2 and OPM 5): swell voltage (line-neutral) $330\,Volt$, CB_2 breaker resistance $R_{on} = 0.01\,Ohm$, snubber resistance $R_s = 1 \times 10^6\,Ohm$, snubber capacitance $C_s = infinite$, and switching time = [0.15 sec 0.35 sec] with NO condition, interruption voltage fault generation (OPM 3 and OPM 6): circuit breaker CB_3 breaker resistance $R_{on} = 0.01\,Ohm$, snubber resistance $R_s = 1 \times 10^6\,Ohm$, snubber capacitance $C_s = infinite$, and switching time = [0.15 sec 0.35 sec] with NO condition; Series-AF: series inductance L_{Se} = 0.0015 mH, MOSFETs (S_1, S_2, S_3, and S_4), FET resistance $R_{on} = 0.1\,Ohm$, internal diode resistances $R_d = 0.01\,Ohm$, and snubber resistances $R_s = 1 \times 10^5\,Ohm$; Shunt-AF: shunt inductance L_{Sh} = 30 mH, IGBTs (S_1, S_2, S_3, and S_4), internal diode resistances $R_d = 0.001\,Ohm$, and snubber resistances $R_s = 1 \times 10^5\,Ohm$; series transformer: rating kVA $1000\,kVA$, frequency $50\,Hz$, Transformation Rating (N_1/N_2) 1 : 1, series ripple filter $C_{se} = 4700\,\mu F$; load impedance $R_C = 1\,ohm$ and $L_C = 0.01\,mH$; non-linier load,): CB_5 ON and CB_4 OFF, rectifier, diodes (S_1, S_2, S_3, and S_4), $R_{on} = 0.001\,Ohm$, forward voltage $V_f = 0.8\,V$, snubber resistances $R_s = 500\,Ohm$, and snubber capacitance $C_s = 250 \times 10^{-9}\,Ohm$; linear load: CB_5 OFF and CB_4 ON; linear and non-linear load: static active and reactive load $P_{SL} = 11\,kW$ and $Q_{SL} = 6\,kVAR$; DC link: DC voltage $V_{dc} = 400\,Volt$; photovoltaic array 1 and photovoltaic array 2: active power $12\,kW$, irradiance$1000\,W/m2$, temperature $25^0\,C$, MPPT perturb and observer; dc-dc boost converter: IGBT internal diode resistances $R_d = 0.001\,Ohm$, forward voltage $V_f = 1\,Volt$, current 10% fall time $T_f = 1 \times 10^{-5}\,Sec$, current tail time $T_t = 2 \times 10^{-5}\,Sec$, snubber resistance $R_s = 1 \times 10^5\,Ohm$; snubber capacitance $= Infinite$, diode (D) $R_{on} = 0.001\,Ohm$, forward voltage $V_f = 0.8\,V$, snubber resistance $R_s = 500\,Ohm$ and snubber capacitance $C_s = 250 \times 10^{-9}\,Ohm$, $C_L = 0.002\,F, R = 0.01\,\Omega$, and $L = 0.01\,H$; proportional integral 1 and proportional integral 2: proportional gain (K_P) 1 and K_P2 =0.2, integral gain (K_I) 1 and K_I2 =1.5; fuzzy logic controller: fuzzy inference system mamdani, composition max-min, defuzzification max-min; input MFs: Error V_{dc} ($V_{dc-error}$) trapmf and trimf, Delta Error V_{dc}, ($\Delta V_{dc-error}$) trapmf and trimf; Output MFs: instantaneous of power losses ($\bar{p}_{loss}$) trapmf and trimf.